Divertor concept for the W7-X stellarator and mode of operation

H. Renner, J. Boscary, H. Greuner, H. Grote, F.W. Hoffmann, J. Kisslinger[1], E. Strumberger[1], B. Mendelevitch[1]

Max-Planck-Institut für Plasmaphysik, Teilinstitut Greifswald, D 17491 GREIFSWALD, Wendelsteinstr. 1, IPP-EURATOM Ass.
[1]Max-Planck-Institut für Plasmaphysik
D-85748 GARCHING, Boltzmannstr. 2, GERMANY, IPP-EURATOM Ass.

ABSTRACT

A favourable property of the stellarator concept is the potential of stationary operation within a magnetic configuration maintained by a superconducting coil system. For proof of principle the stellarator Wendelstein 7-X is presently under construction at Greifswald, Germany, and the start of operation is planned 2006. The magnetic configuration of the confinement is a non-axisymetric 3D configuration with a helix-like magnetic axis and five identical magnetic field periods. As a first step divertor design an open divertor structure has been chosen, which benefits from the inherent divertor property of the magnetic configuration. The system will allow an effective particle and energy exhaust for a wide range of plasma and magnetic parameters. Experimental tools, e.g. localised heating, various heating schemas, gas feed and pellet injection, impurity doping and variation of the pumping speed together with appropriate diagnostics are provided. The purpose is to investigate different modes of operation for the divertor system and to evaluate an extended data base for further improvement of the divertor.
The main heating method will be 140 GHz ECR as a cw heat source of 10 MW. Additional heating schemes are ICRF and NBI.

1. INTRODUCTION

The stellarator concept offers an attractive alternative to the tokamak approach in magnetic confinement fusion. The magnetic field structure, which is required for equilibrium and stability of the confined plasma, is generated by external coil currents only, and has an inherent divertor. The net current free operation eliminates the problem of plasma disruptions and thus favours steady-state operation.
W7-X is a large "advanced stellarator" of the HELIAS-type (R=5.5 m, a=0.55 m, B_o=3 T, five periods, moderate shear and variable rotational transform $5/6 \leq \iota \leq 5/4$ at the boundary) with the aim to demonstrate the reactor potential of this stellarator line at steady-state operation close to fusion relevant parameters [1]. The capability of stationary operation requires the realisation of a super conducting magnet system consisting of 50 modular coils and 20 planar coils, the operation of a 140 GHz ECR cw heat source, the installation of a divertor to handle the power and particle flux and to limit the impurity fraction to tolerable levels. Additional heating schemes, ICRF and NBI, will be provided for flexible experimentation.

2. PHYSICS OBJECTIVES AND OPTIMIZATION CRITERIA FOR W7-X

The physics objectives are met by a proper architecture of the magnetic configuration including modular coils, which takes into account the following optimization principles [2]:

1. Robust magnetic surfaces.

2. Reduced Pfirsch-Schlüter (PS) currents towards $\langle j_{||}^2 / j_{\perp}^2 \rangle < 0.5$ [3].
3. Good magneto-hydrodynamic (MHD) stability up to $\langle \beta \rangle = 5\%$.
4. Minimized deviation of trapped particle drift orbits from the flux surfaces (drift optimization) to reduce the neoclassical transport [4] in the l.m.f.p. regime.
5. Good α-particle confinement in reactor extrapolation.
6. Minimized bootstrap current.
7. Inherent divertor properties.

Consequently, a verification of the design properties, quasi-stationary operation and control of the plasma parameters are the main goals of the experiment. In order to obtain 1) quasi steady state operation in a reactor relevant plasma parameter regime, with temperatures $T_e < 10$ keV, $T_i = 2 - 5$ keV and densities $n_e = 0.1 - 3 \cdot 10^{20}$ m^{-3}, 2) good plasma confinement to improve the data base for reactor extrapolation, 3) stable plasma equilibrium at a reactor relevant plasma $\langle \beta \rangle$ of about 5%, 4) investigation and development of a divertor to control plasma density and impurities W7-X must provide sufficient experimental flexibility. A variation of key parameters such as the magnetic induction, the rotational transform and shear, the edge- and bulk plasma parameters, the magnetic configuration, etc…, should be possible within a wide range. These demands have apparently a strong impact on the shape of the vacuum vessel and require additional coil sets, e.g., planar toroidal field coils to change the rotational transform.
To achieve reliable and relevant data for the further improvement of the stellarator concept quasi-stationary operating conditions are mandatory. The macroscopic MHD time to establish an equilibrium of the confinement - in respect of bootstrap current, current density distribution, etc. - is about 10 seconds, whereas the time constants related to the gas inventory of the wall and impurity flux from the plasma-wall interaction are in the order of minutes. The specification and integration of divertor components has to reflect these needs.
W7-X does not aim at DT-operation, so that provisions for remote handling in radioactive environment are not foreseen.

2.1. Heating systems
The physics objectives of W7-X will be addressed in a staged experimental programme with a staged heating arsenal. In stage I, the experiments will concentrate on the steady-state issue and the related questions on confinement, particle and power exhaust, and control. ECRH will be the main heating system with 10 MW power because of its cw capability and the uncoupling from particle fuelling. ECRH proved its capability for plasma start-up and heating towards the envisaged parameters. NBI and ICRH will be available with somewhat lower power to increase the experimental flexibility. Stage II will concentrate on high β physics and NBI will be upgraded towards 20 MW, which is necessary to reach the β limits at reduced magnetic field and high density.

3. W7-X DIVERTOR

3.1 Magnetic configuration of W7-X
W7-X is a **HELI**cal **A**dvanced **S**tellarator (HELIAS) with a strongly varying plasma cross section, 5 field periods and moderate shear. In Fig. 1a the plasma contour is represented by the LCMS: For one period the related coils are added and the arrangement of the ten proposed divertor units is integrated. 50 non-planar coils provide the confining magnetic configuration. 20 additional planar coils are introduced for experimental flexibility. The non-planar coils system and the two planar coils of one half period is shown in Fig. 1b: The planar coils will

be inclined in relation to the horizontal plane to generate vertical fields for the control of the magnetic axis shift. The calculation of the flux surfaces show a variation from a strong indented elongated shape, or "bean shape", in the $\varphi = 0^{o}$ plane to a triangular shape in the $\varphi = 36^{o}$ plane. Together with the islands at the boundary, parts of the divertor units can be identified.

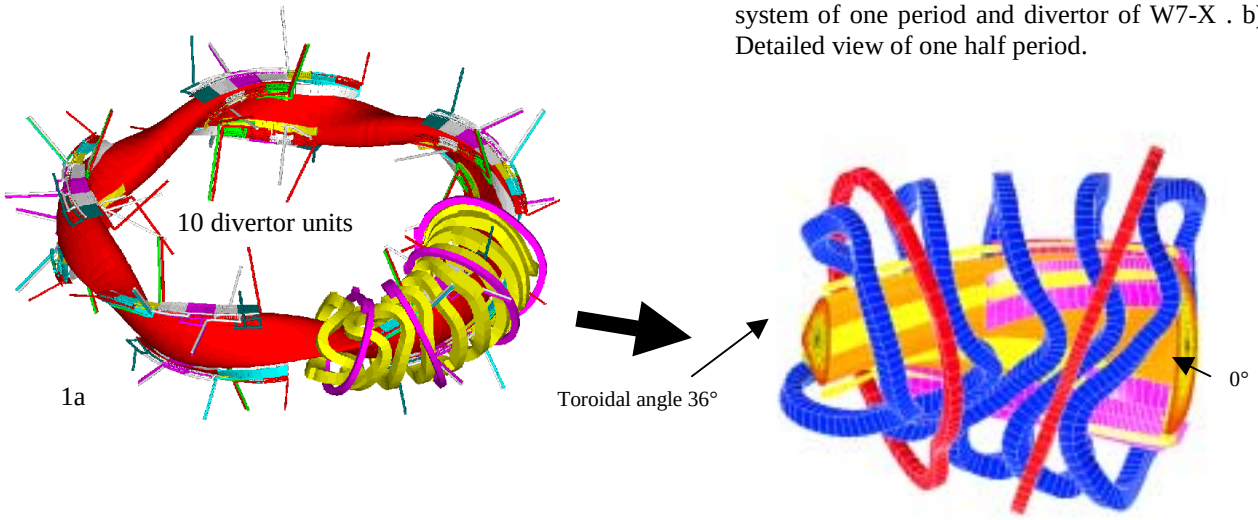

Fig. 1. Coil system and divertor in W7-X.
a) Total view: Plasma contour: LCMS, coils system of one period and divertor of W7-X . b) Detailed view of one half period.

3.2 Properties of the plasma boundary and divertor concept

The confinement region is either defined by the separatrix of islands (being intersected by target plates) or by an ergodised boundary with remnants of islands.

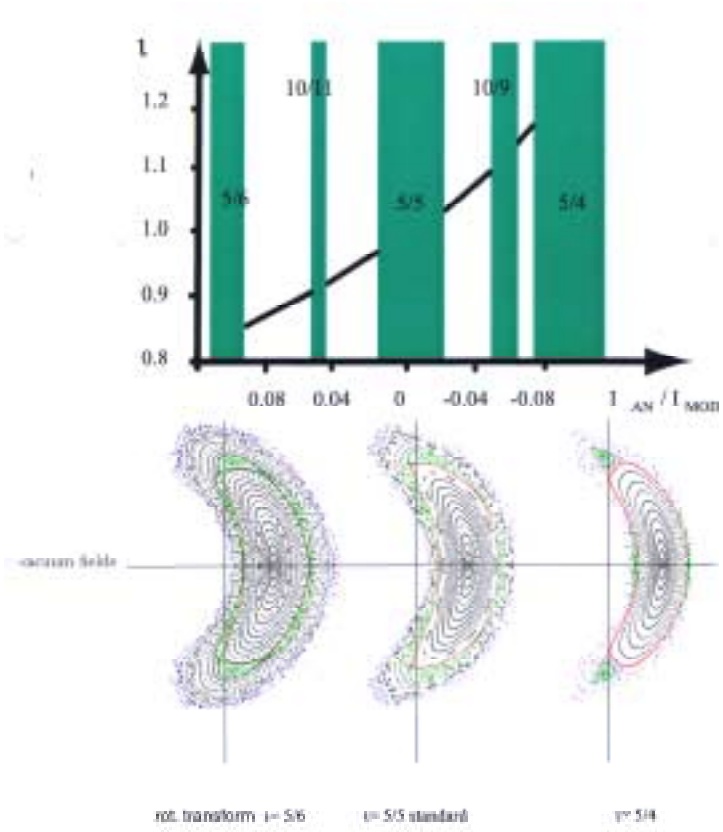

Fig. 2: Variation of the rotational transform: Depending on the current ratio for the ancillary and modular coils the boundary values of the rotational transform can be controlled.
For the rational values: 5/6, 5/5 and 5/4 islands and ergodisation characterise the boundary, indicated by the shadowed areas. These parameter ranges are provided for divertor operation , otherwise limiter operation will be realised.
The Poincaré plots for the vacuum case are correlated: control coils with $I_c=0$ (lower part). Note, islands at the boundary are marked by red points, ergodised areas by blue points.

Unlike in tokamak divertors, the X-lines in island divertors are helical, with the pitch depending on the resonant rotational transform of the island chain. For the standard configuration ($\iota = 1 = 5/5$ at the boundary), five toroidally closed helical X-lines magnetic are present. In the case of extended islands, the positioning of divertor elements along the helical edge (areas with the strongest poloidal curvature of the magnetic surfaces) allows to concentrate the plasma flow from the confinement region in the SOL on target plates and to uncouple the plasma core from the wall completely.

3.3 Divertor modelling

Because of the lack of an elaborated 3D code almost deduced and calibrated from tokomak data banks several methods have been applied to define the specifications and shape the geometry of W7-X divertor components. Such tools are also very valuable for parameters studies, but require particular input assumptions: It requests a combined and iterative execution. For the design of the W7-X divertor the following informations were used:

- Simplified divertor modelling

A simplified SOL model has been used starting from the SOL particle and power balances. For the operating parameters of the W7-X experiment under the assumption of anomalous transport values for the radial decay length of the boundary parameters in the order of 1cm were obtained to define the loading volume for the magnetic flux bundles close to the LCMS. The randomisation of the field lines shows a typical connection length to be 75 m. For the W7-X geometry and typical conditions of operation the parameters are listed in table 1:

major radius R	[m]	5.5
minor radius	[m]	0.55
magnetic field B	[T]	2.5
plasma volume V	[m^3]	30
plasma surface A	[m^2]	120
input power P	[MW]	10
particle flux Γ	[10^{20} s^{-1}]	200
connection length L_C	[m]	75
boundary power density P/A	[MW/m^2]	0.08
particle flux density	[$10^{20} m^{-2} s^{-1}$]	2.5
boundary density n	[10^{20} m^{-3}]	0.2
boundary temperature T	[keV]	0.07
decay length λ_T	[cm]	1
decay length λ_n	[cm]	2

Table 1: W7-X SOL parameters as calculated on the basis of a simple SOL model with anomalous transport characterised by $n^*\chi_e = 1\ 10^{20}\ m^{-1}s^{-1}$ and $n^*D = 0.05\ 10^{20}\ m^{-1}s^{-1}$.

- Field line tracing

The results of 3D ray tracing of the vacuum configuration, also including finite <ß> equilibrium cases at the boundary [5] are used to define the interacting divertor surface pattern (fig. 3). In combination with simulation of perp. transport (a typical transport coefficient is 1m²/s, values up to 10 m²/s were investigated) by Monte-Carlo code the power load was estimated. For all conditions the maximum power load was found to be limited to a value of less than 8 MW/m², as shown for the standard case in fig.4.

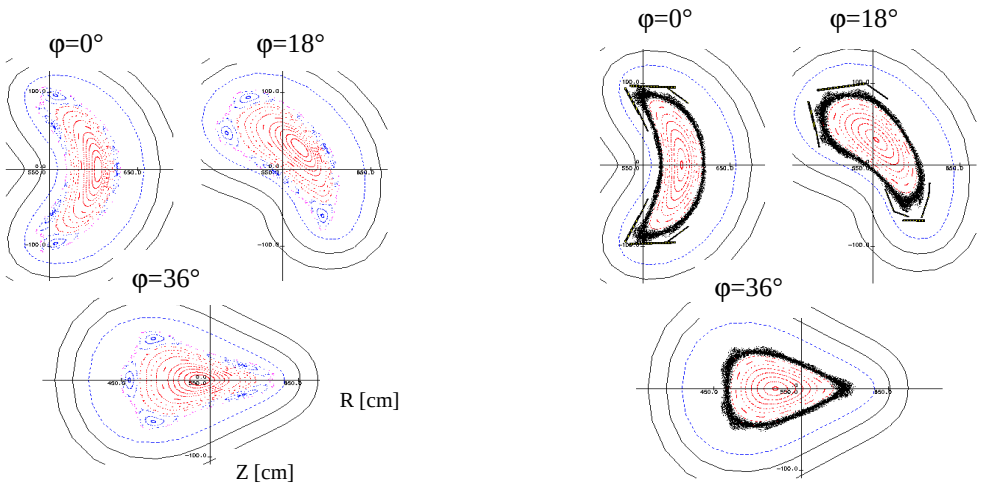

Fig. 3. Poincaré plots of the standard configuration: ι=5/5, β=0 at the cross-section φ=0°, 18° and 36°. On the left side: magnetic surfaces and associated islands. On the right side: Boundary topology for the optimised divertor contour with target and baffle area, simulation of perpendicular transport by "field line diffusion" (D=1m^2/s).

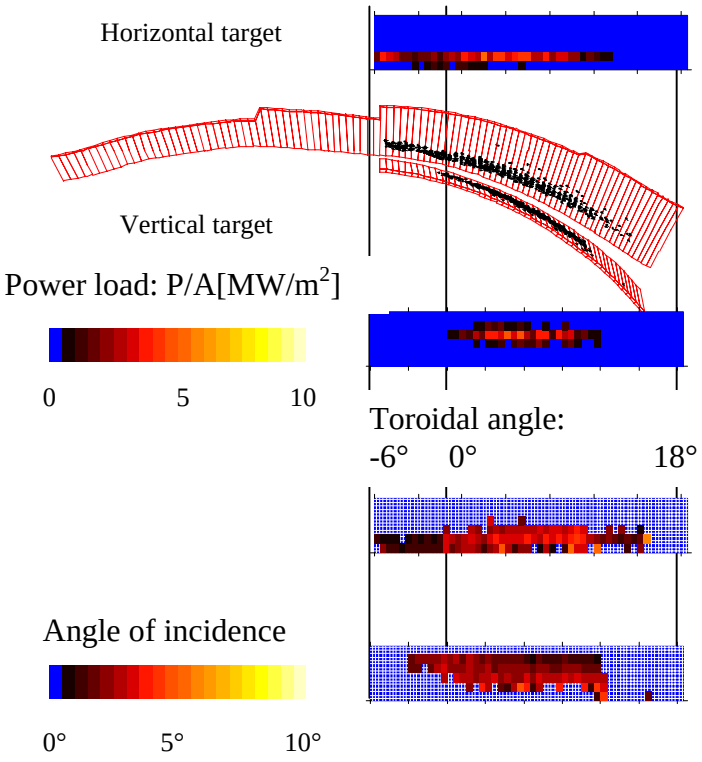

Fig.4
Deposition pattern on the target area of one divertor unit.
Standard case: ι=5/5, β=0 (Fig. 3)
P_{in}=10 MW, no radiation
Transport simulation by field line diffusion.

The target area consists of two target plates. The power densities are indicated on the vertical and the horizontal target plate according to the colour bar between 0 and 10 MW. The angle of incidence of the flux bundles in the range 0 to 10° is shown.

- Plasma parameters at the boundary

Simplified 3D SOL models were evaluated to get information about the temperature and density distribution. For this, the 3D flux topology was combined with 1D fluid models. This method has benefits from the ordering of the open flux bundles outside the separatrix region where only field lines with a long connection length approach close to the separatrix and get significant loading from the confinement area by perpendicular transport [6]. The 1D treatment of the bundles of different length and power and particle flows delivers the plasma parameters along the field lines. Finally, the superposition in 3D geometry lets approximate the 3D temperature and density profiles.

- Influence of plasma pressure on the magnetic configuration

Finite <ß> plasmas modify the boundary. While the vacuum magnetic field can be easily obtained from the external coils using Biot-Savart's law, a new code, MFBE [7], was developed for the computation of finite-β magnetic fields. It evaluates these magnetic fields by using the results of the NEMEC free-boundary finite-β equilibrium code. The sufficiently small shift of the magnetic surfaces and the small change of the rotational transform with increasing β are important properties to guarantee that the target and the baffle plate configurations work without geometrical adjustments for various finite-β equilibria (Fig. 5). The plasma boundaries of the finite-β equilibria lie inside the LCMS of the vacuum field, while the edge region ergodises and the width of the islands normally extends with increasing β. The long (L > 200 m) and intermediate (L = 45-200 m) field lines come close to the LCMS so that most of the power and particles flow along them to the divertor plates. At the standard case, the total size of the wetted area for the long field lines (L > 45 m) is A = 1.9 m^2 for the vacuum case and A = 5 m^2 for <β> = 4%. Simulation of the energy transport across the field lines by "diffusion" of field lines leads to a further increase of these intersection areas.

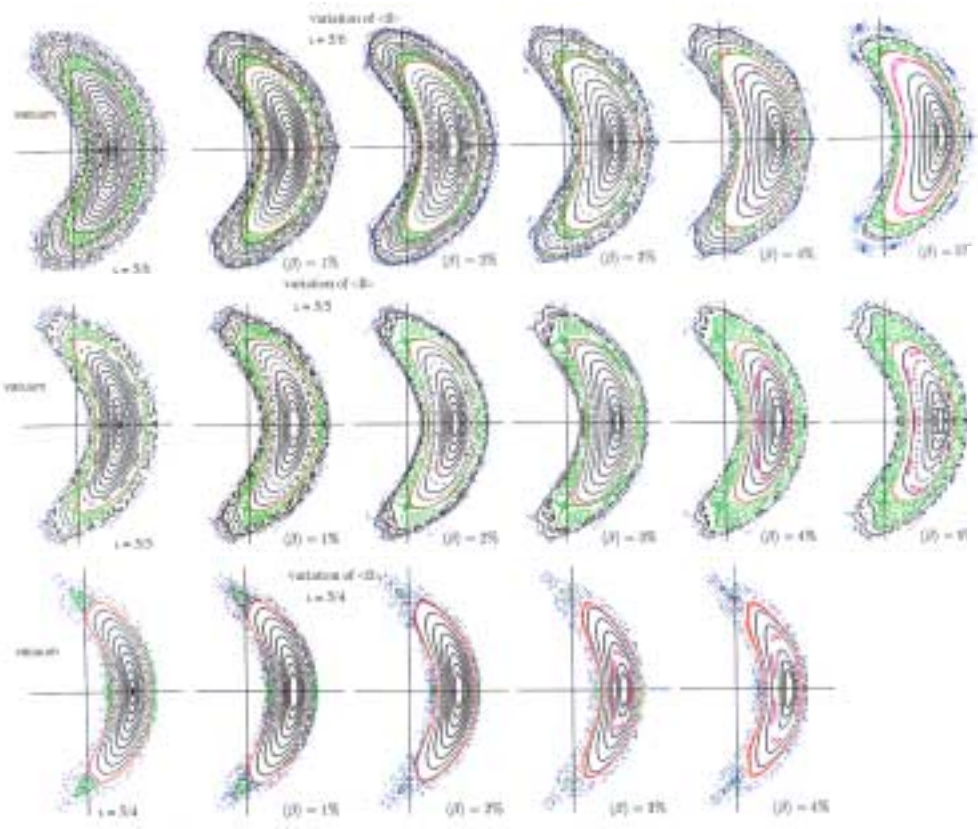

Fig. 5: Poincaré plots: Variation of ι and β.

Magnetic surfaces are indicated by black dots, islands by green dots, ergodised field lines by blue dots.

For the target geometry of W7-X the LCMS is marked by red dots.

Distributed over one divertor unit the results of field line tracing with transport simulation are presented in Fig. 6. Whereas for the improved equilibrium with low Shafranov-shift the variation of the ß has relatively small influence on the pattern, the rotational transform and the consequent modification of the flux topology in the SOL needs a large extension of the target area: The wetted area in all cases is of the order 2-5 m^2. The total area has to be increased to 27 m^2 in order to control the power deposition on the target surface for the wide range of magnetic and plasma parameters of the planned experiments.

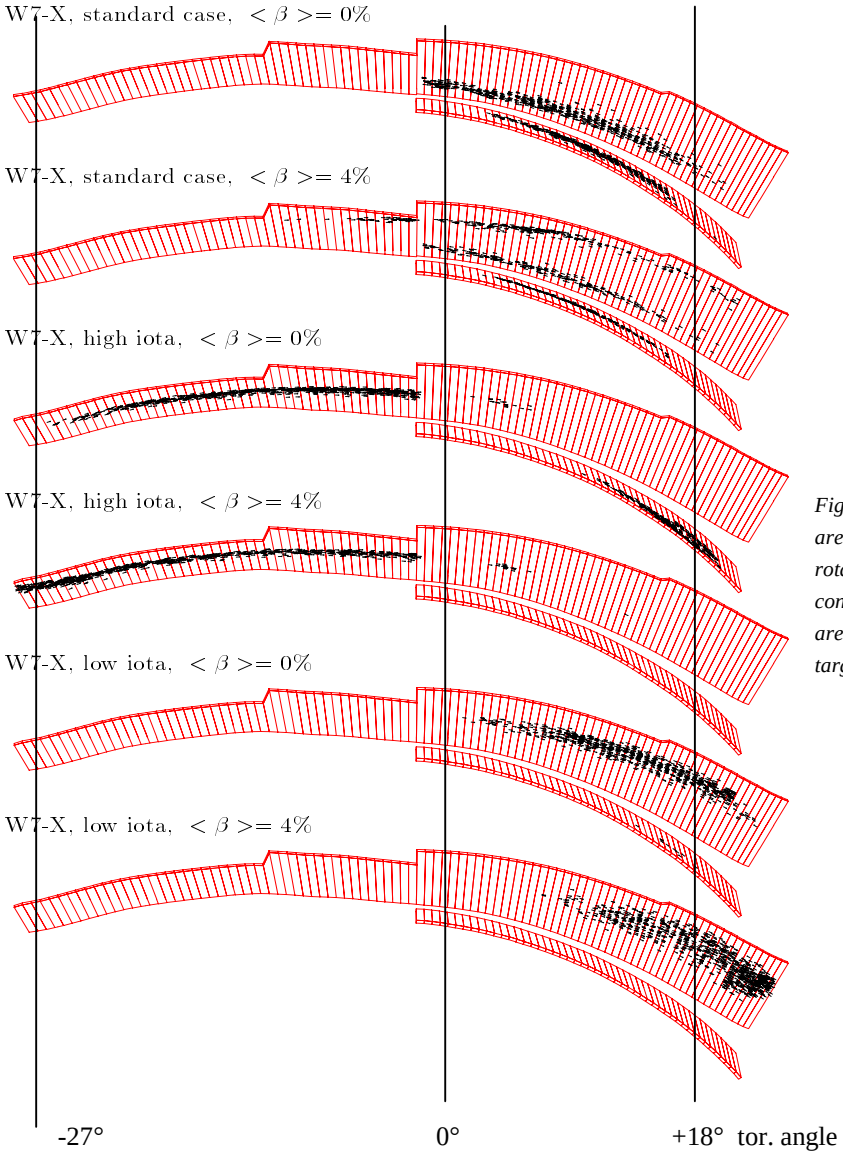

Fig. 6: Calculated deposition pattern on the target areas of one divertor unit depending on <ß> and rotational transform. The two target plates, which consist of single target elements, of one divertor unit are shown. The toroidal angle (Fig. 3) along the target is indicated

- Ergodisation

For example, the high-ι vacuum and finite-β case was studied in detail: the magnetic fields of W7-X are characterised by 5/4 island remnants embedded in a stochastic region outside the LCMS. Mapping of the magnetic fields for <β> = 0, 2 and 4% shows reduction of the 5/4 island remnants with increasing β, i.e., the stochasticity is increased in the edge region. In order to quantify the stochasticity, bundles of field lines forming flux tubes are traced in this region taking into account the geometry of the plasma-facing components, i.e., the divertor, target, baffle, side plates and the first wall [8]. Because of the exponential scattering of close field lines in a stochastic field, the circumference of the area enclosed by a flux tube increases

exponentially. Calculating this circumference as a function of the length of the flux tube yields the Kolmogorov length L_K, which measures the stochasticity. By comparing the Kolmogorov lengths of flux tubes with their corresponding connection lengths L_c to the plasma-facing components, two transport regimes are distinguished, namely, the stochastic transport region with $L_C > L_K$ and the laminar transport region with $L_C \leq L_K$, where the parallel transport is the dominant feature. Averaging over all Kolmogorov lengths yields $L_K \approx$ 57 m for the vacuum case. L_K increases with increasing ß: For <ß> = 4% $L_K \approx$ 37 m is obtained, that is the stochasticity is really increasing with <ß>. The outermost part of the stochastic area can be characterised with diffusivities of $\chi_{erg} > 3.5$ m^2/s.

- Application of B2 code

The multi-fluid code B2 [9] was adapted to describe the SOL parameters. Since B2 is a 2D code the geometry of the boundary was averaged (distances) and integrated (areas and volumes) in the toroidal direction. Significant unloading of the target plates is predicted by radiation losses of C impurities [10]. A high recycling mode seems possible for relatively low separatrix densities above 2 10^{19} m^{-3}.

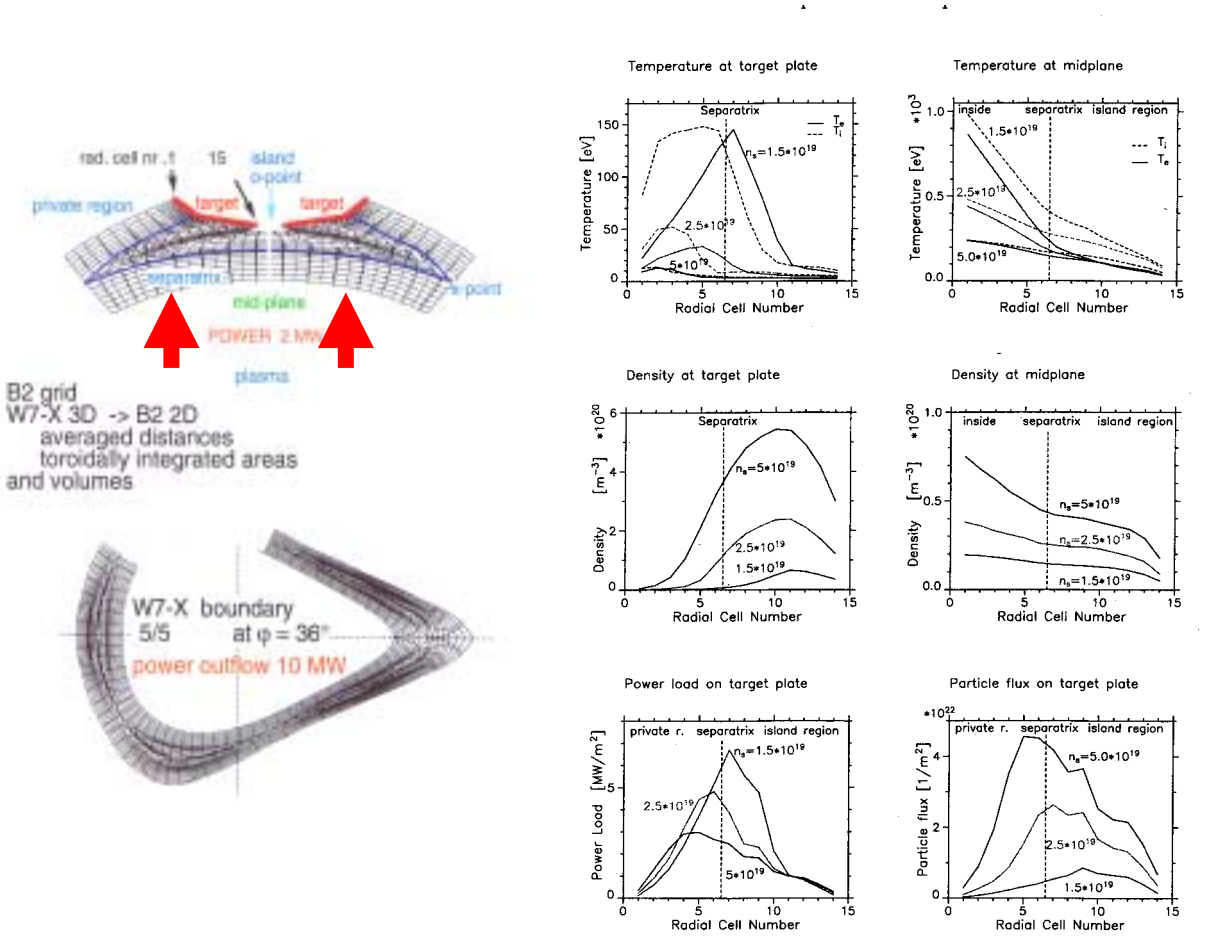

Fig. 7: Results of B2 code estimates. For the W7-X 3D configuration the code becomes applicable with averaged distances and toroidally integrated areas and volumes. On the left side the used mesh is described: In the standard case of W7-X five island chains are present. For a total input power of 10 MW only 2 MW are related to one island chain in respect of the symmetry condition. For the corresponding cell numbers main parameters are evaluated: Density, temperature on the target and midplane, and power density and particle fluxes on the target depending on the separatrix density for D_2 operation.

- Orbit losses, deposition on plasma facing components

A code package was evaluated to compute plasma equilibria, the corresponding fields inside and outside the plasma boundary, particle losses taking in account pitch angle scattering and slowing down, and the deposition patterns of lost particles on plasma facing components. The losses of fast ions (65 keV deuterons, 3 MeV protons and 1 MeV tritons) and their deposition patterns on plasma facing components are studied. Most of the lost counter-injected deuterons which carry the major part of the lost energy hit the divertor target plates, while only a small fraction of particles [11] is interacting with the wall.

- EIRENE, neutral particle balance

The position of the pumping gap and the geometry of the baffle plates was optimised on the basis of 3D neutral particle studies by means of the EIRENE code [12]. The concentration of the neutral particles close to the target plates and the improvement of the pumping efficiency were intended.

- 3D self consistent modelling of the plasma boundary

First attempts to analyse the complex boundary physics of W7-AS, the precedent device of W7-X, using the 3D plasma transport EMC3 (Edge Monte Carlo 3D) have been started with promising results [13]. The Greifswald stellarator physics group is progressing with the development of a 3-D plasma fluid model based on the W7-X topology where strong stochastic effects become important [14].

4. DIVERTOR DESIGN

The installation of the divertor must take into account the particular geometry of the vacuum vessel and the requirements of the heating and diagnostic systems. The main plasma parameters during divertor operation are listed in table 2.
In respect of the structure of the plasma boundary 10 divertor units, two per field period, have to be arranged to avoid leading edge problems. The in-vessel components of W7-X are:

- the Plasma Facing Components (PFC): targets, baffles, wall protection
- the control coils
- the pumping system, including cryopanels.

Power, stationary peak power	**10 MW** 20 MW for period of 10s
particle flux (external source) NBI gas puffing pellet injection	 $\mathbf{\Gamma_{NBI} < 10^{21}\ s^{-1}}$ $\Gamma < 10^{22}\ s^{-1}$ $\Gamma < 10^{22}\ s^{-1}$
particle flux (internal source) $\tau_{p\sim}$0.5 s for $N_{max} = 10^{22}$ estimate of maximum fluxes related to the input power of 10 MW: (convective power to targets per electron-ion pair: $P_d = \gamma \Gamma kT_d$; with γ=8 and kT_d=10 eV)	 $\Gamma \leqslant 2\ 10^{22}\ s^{-1}$ $\Gamma \leqslant 8\ 10^{23}\ s^{-1}$

Table 2: Operational parameters of the W7X divertor

4.1. Target plates

As shown in Fig. 6, the power load deposition on the target plates depends on the magnetic and plasma parameters. The positioning of target plates is optimised according to the following criteria:

• Concentration of the plasma outflow on the target plates, and separation of the plasma from the vessel.

• Power load up to 10 MW/m^2 limiting the angle of incidence of field lines on the targets to a value below 1-3°.

• Compatibility with the variation of the magnetic configuration: rotational transform with values $5/6 \leq \iota \leq 5/4$.

The target plates are designed to withstand a heat flux up to 10 MW/m^2 and a maximum total load of 10 MW for steady state operation [15]. Ten divertor units, i.e., two units per period, have been shaped to follow the stellarator symmetry. Each unit consists of two smooth sets of target plates for high power load and a baffle designed for low power load adjacent to each plate. The 3D ideal target surface is approximated by flat standardised target elements. The single target elements are standardised and seven different types are foreseen. The averaged width is 55 mm and the length between 270-500 mm. Flat carbon fibre tiles are brazed or welded on the cooling structure. Presently, the combination of CFC NB31 combined with a water cooled CuCrZr heat sink is favoured.

10 to 14 single target elements are assembled to modules with cooling manifold and mounted on a common support structure. These elements are actively cooled by the pressurized water flow. Thus, one divertor unit consists of 130 target elements (1/10 of the total value), which span an area of 2.7 m^2.

4.2. Baffle and wall

The divertor units are completed by the integration of baffles and cryopumps for efficient pumping under stationary conditions dealing with external fluxes of 5 10^{21} 1/s (NBI, pellet, gas feed etc.) and pressures in the range of up to 10^{-3} mbar in the divertor.

The baffle elements, covering 3 m^2 per divertor unit, are designed to withstand a power load of $P/A < 0.5$ MW/m^2 with integrated cooling circuits whereas the wall elements are specified for $P/A < 0.2$ MW/m^2. Alternative concepts are presently studied and prototypes are manufactured and tested:

1. Panels with surface layers of B_4C, Si, etc..., generated by plasma spray technique [1]. For the protection of the inner wall contour 150 individual elements are needed per period. A baking temperature of 150 °C is foreseen.
2. clamped C tiles on water cooled supporting structure.

To satisfy the particular requirements of the various heating schemes, ECRH, NBI and ICRH, to adapt the local geometrical constrains, a combination of the various concepts will become necessary.

4.3. Pumping

The pumping installation will consist of two independent systems. To be flexible in respect of the neutral particle pressure inside the divertor and to allow the use of additional particle sources for control of plasma parameters, turbomolecular pumps (TMPs) and additional cryopumps with high pumping speed will be installed.

TMPs with their corresponding backing pumps, installed on the 10 divertor boxes will define the basic pumping system of W7-X. The pumps will also be used for pumping the divertor box during the discharge with acceptable pump speed. One unit will consist of suitable TMPs with an effective pumping speed for H_2 of 4200 l/s at the divertor box, 1000 m^3/h roots- and 65 m^3/h mechanical pump.
Two symmetrical pumping ducts connect the TMP with the divertor box. In these pumping ducts butterfly valves can be used to modify the pump speed. The base pressure will be less than 10^{-8} mbar.
The cryopanels are positioned inside the vessel, between the diagnostic ports. 4 cryopanels per divertor unit will be installed. The cryopump system can be operated with high flexibility in relatively short cycle time for recovery and offsets the disadvantages of restricted pumping capacity. The high pumping speed can be maintained during pulses lasting up to two hours. By special conditioning (Ar, active C) even for He an interesting pumping rate can be achieved. Including the TM-pumps a total pumping speed of 190 000 l/s will be provided.

4.4. Control coils

Control coils are integrated in the divertor units. The system consists of two current coils in each field period. In respect of the symmetric positioning and the achieved "resonance" effect already the superposition of relatively small fields to the magnetic configuration is sufficient. The main features of the control coils are:

• To control the variation of the connection length and modify the distance between target plates and separatrix by changing the island size at the boundary.

• To compensate error fields.

Compensation of symmetry-breaking error fields, e.g. due to small construction inaccuracies of the device. Error field compensation is achieved by an individual choice of current in each control coil.

• To shift and spread the power deposition on the target plates.

If the diffusive broadening of deposition areas on the targets is too small to prevent excessive power load, the control coils can be used to sweep the strike points on the targets. Currents of 10 kA*turns shift the strike points on the target plates about 5 cm poloidally. Additionally to the variation of the deposition pattern a sweeping effect is introduced when energising the coils by AC currents. In that case the transient magnetic field of the control coils oscillates the strike points on the target plates.

4.5. Divertor engineering strategy

The divertor components will be mounted on the inner vessel wall. The tolerances for positioning of the critical target plates are: alignment within 0.5° related to the horizontal plane, radial displacement less than 2 cm. For limiter operation a higher accuracy with tolerances on the order of mm has to be achieved. The problem of thermal movement and deformation of the vessel, and, in respect of the magnetic configuration, the geometrical displacement of components supported by the vessel will be solved by the thermal control of the cryostat temperature. For that purpose an additional water-cooling circuit with a small capacity of 300 kW is needed to compensate the heat transfer to the cryostat from the plasma facing wall, which has to be specified for a power exhaust of up to 10 MW with an average power load of 100 kW/m^2. For control of the particle balance stationary plasma operation at first wall temperatures up to 150° C will be possible at temperatures of even less than 60° C for the cryostat.

For safe operation of the divertor components operational diagnostics, thermography, thermometry, flow control, measurements of thermo-currents, will be installed.

Supplementary sophisticated diagnostics will be used to define the plasma parameters of the boundary and at the interacting areas.

5. MODE OF OPERATION

The variability of the magnetic parameters, especially, rotational transform, shear, ripple and magnetic well allows investigations of the confinement, equilibrium, stability, transport. The different heating schemas give many possibilities for variation of the plasma parameter, covering the LMFP with low collisionality up to high densities, achievement of high β, local power deposition, local current drive, modification of particle energy distributions, transport associated generation of electric fields and study of bifurcations (Table 3).

5.1. Experimental range for divertor

5.1.1 Geometry of the SOL

The second step divertor improvement will be based on data from experiments with variation of the SOL: e.g. importance of the magnetic connection length L_c of the open flux bundles and distance of the LCMS from the target surface L_N by means of the magnetic parameters and the control coil. Additionally, the plasma pressure, application of vertical fields will modify the deposition pattern on the target. Transitions between boundary control by limiter operation, islands with variable symmetry and ergodisation can be explored in W7-X.

5.1.2. Energy exhaust

The capability of the target plates is designed for an energy exhaust of 10 MW in stationary operation for convective plasma losses. A reduction of the local power deposition density can be achieved by the application of the sweeping technique with frequencies up to 20 Hz. The deposition pattern on the target will be widened by almost a factor of 2 –3, whereas the thermal time constant of the target is in the order of few seconds. Estimates of the radiative losses, even with impurity seeding and detached cases, indicate a significant unloading and more homogeneous loads on the total plasma facing surface of the vessel. Therefore, the capabilities for heat removal of the baffle and wall protection areas have been designed correspondingly.

5.1.3. Particle exhaust

The use of 10 individual divertor units of divertor system allows unique experiments concerning neutral behaviour, impurity migration by active control of gas feed and local pumping efficiency.

Maximum fluxes up to 10^{23} electron-ion-pairs per second, associated with the convective power source of 10 MW, are expected at the targets with temperatures of less than 10 eV. The particle flow across the last closed magnetic surface (LCMS) depending on the density range and the confinement is estimated to be several 10^{22} particle s^{-1}. External fluxes by NBI, localised gas puffing and pellet injection in a range up to 10^{22} particle s^{-1} will be applied for heating and control of the density profiles.

For the divertor units the position of the pumping gap and the geometry of the baffle plates was optimised on the basis of 3D neutral particle studies by means of the EIRENE code improving the concentration of the neutral particles close to the target plates and the pumping efficiency .

For particle exhaust two independent systems will be used. To be flexible with respect of the neutral particle pressure inside the divertor and to allow the use of additional particle sources for control of plasma parameters high pumping speed will be installed.

W7-X **"OPEN DIVERTOR EXPERIMENT"**	**VARIATION OF SOL PARAMETERS:** **L_C, L_N, n,** n_{imp}, n_o, **T**, FLUXES AND VOLUME
Magnetic parameters: Rotational transform, shear, magnetic ripple, magnetic axis **control coils**	Structure of magnetic configuration, symmetry of boundary: Limiter/separatrix, "islands, ergodisation **L_C, L_N,** deposition pattern on targets, SOL profiles
Different heating scenarios: **ECRH**, NBI, ICRH	plasma parameter, SOL parameter, modification of shear by **ECCD** **variable deposition profiles, modification of T_e/T_i,** LMFP regime: low $\nu*$, high density, radiation, mass flow by NBI bifurcation of fluxes/**electric fields** influence of **thermo-currents**
Controlled gas feed at variable positions: Target, divertor unit, vessel **Impurity doping** **Pellet injection**	Effect of neutrals: balance, losses **Radiation, detachment** **Migration of impurities** between plasma and divertor units
Control of pumping speed for each divertor unit: TMP, cryo panels (Ar frosting for He)	Screening efficiency, control of radiative boundary He simulation and "ash removal"
Conditioning, **in-situ conditioning**	Plasma wall interaction, gas inventory during stationary operation

Table 3: First step: Open divertor. Experimental features of W7-X and topics of the divertor programme

Special diagnostics for each divertor unit, e.g. calibrated fast gas valves, total pressure gauges, Penning gauges to discriminate between D_2 and He and mass spectrometers will be provided to evaluate neutral and impurity particle flows during the experiment.

5.2. Operational ranges for the plasma boundary

The external control of the magnetic parameter, the minimised pressure dependence of the configuration (bootstrap current, Shafranov-shift) and the absence of disruptive instabilities will open a wide operational field to understand the physical phenomena at the boundary (Table 4). On the other side, the real 3D situation in the stellarator causes a lot of difficulties for the diagnostics and the interpretation of data. If the symmetry conditions can be approached by appropriate positioning of the divertor units in respect of the realised magnetic within narrow tolerances some similarities and correspondences may be used for evaluation of relevant data from local measurements.
Three interesting regimes can be explored :

1. At low collisionality the plasma flow at the boundary will follow mostly the topology of the flux bundles, the deposition on targets is controlled by parallel conduction influenced by perpendicular modifications and electric fields. The plasma temperature on the targets may stay at a high level with small gradients along the field bundles in the direction to the separatrix.
2. With increasing density the temperature will drop. Consequently, a reduction of the impurity sources and a better screening of impurities is expected. The high neutral flux close to the targets will increase the neutral density and hence improve the pumping efficiency.

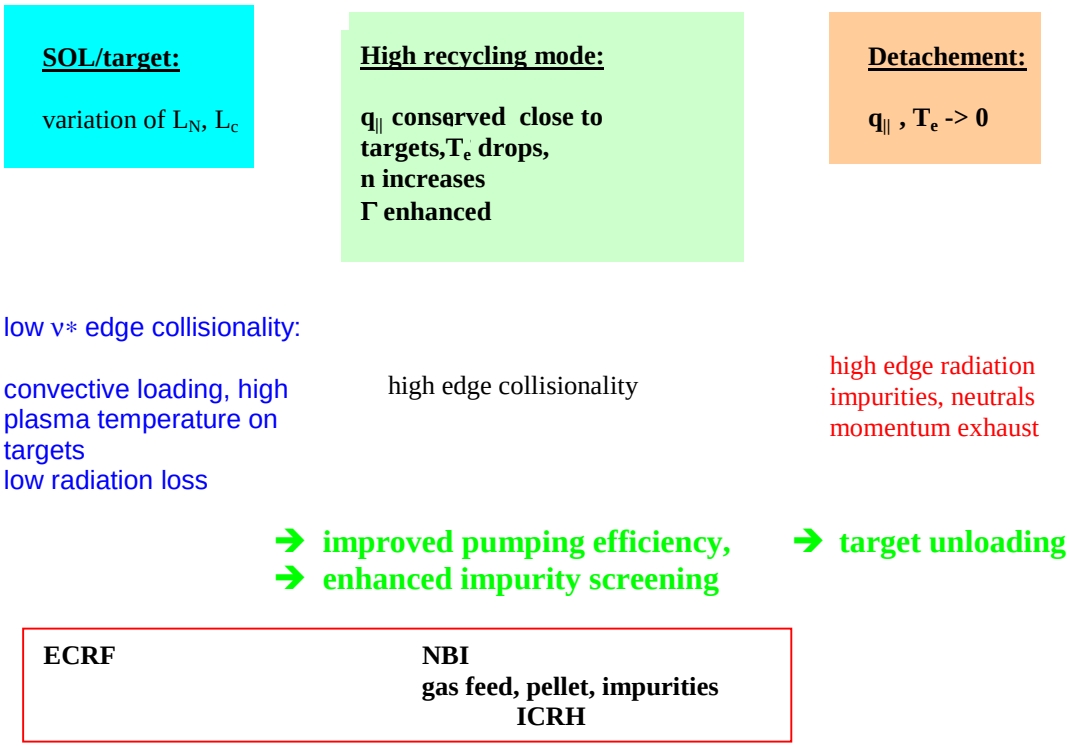

Table 4: Operational range for the divertor experiment in W7-X

3. Depending on the input power high impurity concentration and plasma density at the boundary leads to detachment and significant unloading of the targets. Together with the reduction of T and q the momentum balance has to be satisfied by strong interaction with neutrals. The 3D structure with different connection length of particular flux bundles connected to individual targets will become important for the appearance of asymmetries and the location of detached areas. There is the danger, that the pumping efficiency may by reduced and the control of the particle balance may become critical.

Recent results of the first W7-AS experiments with an island divertor arrangement are very promising and in good agreement with predictions [16].

6. CONCLUSIONS

The stellarator Wendelstein 7-X is designed for steady-state operation. Within a wide range of magnetic parameters, using different heating scenarios with possibilities of current drive, gas feed, pellet injection the optimised properties of the HELIAS configuration will be proven. The divertor design will become an important tool to control the plasma parameters during stationary operation.

In the first step an “open divertor” system with a stationary input power of 10 MW is designed to be integrated inside the inner cryostat vessel. As plasma facing material C, B_4C, low Z material will be used. Three loading areas with different heat load can be identified: target areas with 10 MW/m^2, baffle areas with 0.5 MW/m^2 and wall area with 0.2 MW/m^2. Various concepts have been developed to meet the requirements of heating and diagnostics. Prototypes of target elements capable to withstand a power load of 10 MW/m^2 were already successfully tested [17].
The optimisation of the divertor geometry is based on the field line tracing for the vacuum configurations and the simulation of perpendicular transport by "field line diffusion"
(Monte-Carlo code) to calculate the power deposition on the targets, whereas the pumping efficiency is estimated by the EIRENE [11] code. Local power densities up to 8 MW/m^2 on the target plates were obtained for a wide range of magnetic parameters for the worst case at low-density and high-temperature operation. Studies by means of the B2/EIRENE code demonstrated a significant unloading of the targets by radiation, especially taking into account low-Z impurities. The deposition area changes depending on the twist and symmetry of the x-lines, but in all cases the target areas remain the interacting surfaces for the open peripheral flux bundles. With increasing plasma pressure and higher rotational transform the stochastic edge region of W7-X is widening
The divertor design of W7-X provides a flexible solution of the energy and particle exhaust of a HELIAS device [18]. Unique features to study plasma boundary and transport are included. The variation of the magnetic configuration and the control of the neutral particle balance (by pumping, gas feed) are valuable tools for investigations of the physical phenomena at the boundary to optimise the operation with respect to a reduction of impurity reflux and of power load to the target plates during long pulse discharges. In stellarators without MHD limitations by disruption - operation at high densities and high radiative losses will be favoured and may allow a significant reduction of the power load to the target plates.

REFERENCES

[1] H. Renner et al., Nucl .Fusion 40(2000), p. 1083-1093
[2] G. Grieger, W. Lotz, P. Merkel, J. Nührenberg, J. Sapper, E. Strumberger et al., "Physics Optimization of Stellarators", *Physics of Fluids*, B4 (1992), 2081 – 2091
[3] J. Nührenberg and R. Zille, *Phys. Lett.*, **114A**, 129 (1986)
[4] J. Nührenberg and R. Zille, *Phys. Lett.*, **129A**, 113 (1988)
[5] E. Strumberger, Contr. Plasma Phys. 38 (1998), 106
[6] E. Strumberger, Nucl. Fusion 36 (1996), p. 891-908
[7] E. Strumberger, IPP-report 2/339 (1997)
[8] E. Strumberger, Nucl. Fusion 37 (1997), p.19–27
[9] B.J. Braams, Ph.D. Thesis, Rijksuniversiteit Utrecht (1984)
[10] H. Renner et al., Journ. Nucl. Mat. 241-243 (1997), p. 946-449
[11] E. Strumberger, Nucl. Fusion Vol. 40 (2000), 1697-1713
[12] D. Reiter, Jülich Report 1947, Jülich (1 984)
[13] F. Sardei et al., Journ. Nucl. Mat. 241-243 (1997), p. 135-148
[14] M. Borchardt, J. Riemann, R. Schneider, X. Bonin, Journ. Nucl. Mat. 290-293 (2001), 546-550
[15] H. Greuner, Bitter, W., Kerl, F., Kißlinger, J., Renner, H., *Proc. 18th SOFT*, Karlsruhe, Germany, (1994) 1, 323.
[16] P. Grigull et al., “First island divertor experiments on the W7-AS stellarator”, to be publ. EPS (2001), Madeira
[17] H. Greuner et al., Proc. 20th SOFT, Marseille (1998), Vol. 1, 249
[18] J. Boscary et al., Physica Scripta T91 (2001), 90-93